

N,C-Capped Dipeptides with Selectivity for Mycobacterial Proteasome over Human Proteasomes: Role of S3 and S1 Binding Pockets

Gang Lin,^{*,†} Tamutenda Chidawanyika,[†] Christopher Tsu,[‡] Thulasi Warriar,[†] Julien Vaubourgeix,[†] Christopher Blackburn,[‡] Kenneth Gigstad,[‡] Michael Sintchak,[‡] Lawrence Dick,[‡] and Carl Nathan^{*,†}

[†]Department of Microbiology and Immunology, Weill Cornell Medical College, 1300 York Avenue, New York, New York 10065, United States

[‡]Millennium Pharmaceuticals Inc., 40 Landsdowne Street, Cambridge, Massachusetts 02139, United States

Supporting Information

ABSTRACT: We identified N,C-capped dipeptides that are selective for the *Mycobacterium tuberculosis* proteasome over human constitutive and immunoproteasomes. Differences in the S3 and S1 binding pockets appeared to account for the species selectivity. The inhibitors can penetrate mycobacteria and kill nonreplicating *M. tuberculosis* under nitrosative stress.

Unique features of enzymes from different species can provide a structural basis for the development of species-selective inhibitors, even when the enzymes are highly conserved. Proteasome 20S core particles, which are found in all three kingdoms of life, contain 14 copies each of α and β subunits that form a barrel-shaped complex of four rings ($\alpha\text{-}\beta\text{-}\beta\text{-}\alpha$).¹ Eukaryotic proteasomes that are widely and constitutively (c-20S) expressed have seven different copies of α and β , respectively, but only three of the β subunits ($\beta 1$, $\beta 2$, and $\beta 5$) are enzymatically active. Humans also express an immunoproteasome (i-20S) constitutively in immune cells and inducibly in other cells in response to certain cytokines.² In i-20S, $\beta 1$, $\beta 2$, and $\beta 5$ are replaced by $\beta 1i$, $\beta 2i$, and $\beta 5i$, respectively, which causes changes in many aspects of the immune response, indicating the importance of i-20S in the immune system.³ In contrast, eubacterial proteasomes have usually only one and rarely two types of α and β subunits, and all of the β subunits are active. *Mycobacterium tuberculosis* (Mtb) is the only known bacterial pathogen with a proteasome. The Mtb genes *prcB* and *prcA* encode the β and α subunits, respectively.⁴ The Mtb proteasome plays vital roles in defense of the pathogen against nitrosative stress *in vitro*⁵ and in persistence in mice.⁶

New drugs are needed that can kill nonreplicating populations of Mtb, against which few existing drugs are active.⁷ In our initial pursuit of inhibitors that are selective for Mtb proteasomes over human proteasomes, we exploited structural differences⁸ in the S1 binding pockets and identified peptide boronates whose P1 amino acids confer modest selectivity (up to 8-fold) for Mtb20S over human c-20S.⁸ We then identified 1,3,4-oxathiazol-2-ones with up to 1300-fold species selectivity, which appeared to depend on a unique mechanism involving induction of a conformational change in the Mtb proteasome.⁹ Inhibition of the Mtb proteasome is bactericidal in Mtb that has been rendered

nonreplicating by sublethal levels of reactive nitrogen intermediates,^{5,9} an important component of host defense against Mtb.^{10,11} The instability of the oxathiazolones in serum (see below) spurred efforts to find new pharmacophores that are active on the Mtb proteasome but spare both the human constitutive proteasome and immunoproteasome.¹² Recently, crystal structures of mouse c-20S and i-20S were solved, and a comparison showed that the S1 binding pockets of the $\beta 5$ and $\beta 5i$ subunits are different enough to allow the design of inhibitors that are selective for i-20S over c-20S.¹³ Herein we report a new class of inhibitors that selectively inhibit the Mtb proteasome over human proteasomes by taking advantage of structural differences in both the S1 and S3 binding pockets in Mtb20S versus both human c-20S and i-20S.

A library of 1600 N,C-capped dipeptides was constructed by varying P4 (the N-cap), P3 and P2 (using natural or unnatural amino acids), and P1 (the C-cap).¹⁴ Kinetic studies indicated that this class of compounds act as rapid-equilibrium, reversible, and competitive inhibitors of human proteasomes. X-ray crystallography of the complex of one such compound, ML16 [Figure S1 in the Supporting Information (SI)], with the yeast 20S proteasome confirmed that the C-cap projects into the S1 binding pocket (Figure 1), the first amino acid residue occupies

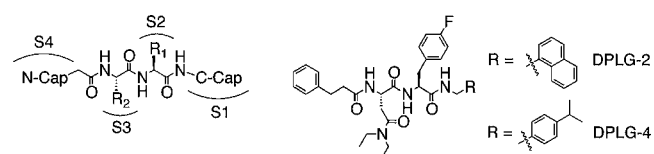
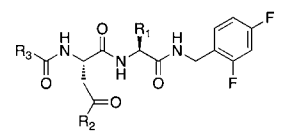


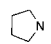
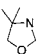
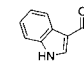
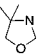
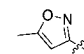
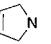
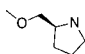
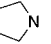
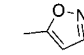
Figure 1. Illustrations of (left) N,C-capped dipeptides and corresponding binding subsites and (right) structures of DPLG-2 and DPLG-4.

the S2 pocket, and the second amino acid residue occupies the S3 pocket.¹⁴ We screened this library against the Mtb20S open-gate (OG) mutant. Of the 1600 compounds tested, 65 exhibited $\geq 80\%$ inhibition of purified recombinant Mtb20SOG at 2 μM . For 60 of these, half-maximal inhibitory concentration (IC_{50}) values were determined by monitoring the hydrolysis of succ-LLVY-AMC by Mtb20SOG at 37 $^{\circ}\text{C}$. The IC_{50} values were then

Received: January 15, 2013

Published: June 19, 2013

Table 1. K_i Values and Species Selectivities of N,C-Capped Dipeptides against Mtb20SOG and Human c-20S


ID	R ₁	R ₂	R ₃	K_i (μM) - β5c (Ac-WLA-AMC)	K_i (μM) - Mtb (Suc-LLVY-AMC)	$\frac{K_{i(\beta\text{5c})}}{K_{i(\text{Mtb})}}$
ML1	4-F-Bn	N(Et)(^t Pr)	PhCH ₂ CH ₂	2.14	0.028	77
ML2	4-F-Bn		PhCH ₂ CH ₂	3.63	0.030	121
ML3	4-F-Bn		PhCH ₂ CH ₂	3.00	0.038	79
ML4	4-F-Bn	neopentylamino		0.003	0.041	0.1
ML5	H		PhCH ₂ CH ₂	10.74	0.042	256
ML6	4-F-Bn	N(^t Pr)(Pr)	PhCH ₂ CH ₂	0.67	0.042	16
ML7	H	N(Et)(^t Pr)		5.01	0.057	88
ML8	4-F-Bn		PhCH ₂ CH ₂	40.68	0.058	701
ML9	4-F-Bn	NEt ₂	PhCH ₂ CH ₂	> 100	0.063	> 1590
ML10	4-F-Bn	neopentylamino	PhCO	0.003	0.063	0.05
ML11	4-F-Bn	NH ^t Bu	PhCH ₂ CH ₂	0.47	0.068	6.8
ML12	4-F-Bn		PhCH ₂ CH ₂	8.40	0.070	120
ML13	H			29.43	0.071	415

converted to inhibition constants (K_i) using the equation $K_i = \text{IC}_{50}/(1 + [S]/K_M)$, where $[S]$ is the substrate concentration and K_M is the Michaelis constant (Table 1). Of these, six compounds had >100-fold, two had >500-fold, and one had >1000-fold selectivity for Mtb20SOG over the human constitutive proteasome β5 (β5c) subunit, and 13 compounds showed potencies of <100 nM. The most potent shared several features: P1 = 2,4-difluorobenzyl as the C-cap; P2 = 4-fluorophenyl; P3 = an Asn derivative; and P4 = 3-phenylpropanoyl as the N-cap. The most species-selective compounds shared a common feature, namely, a fully substituted N atom on the P3-Asn amide side chain, in contrast to the preference of human 20S for the secondary amide neopentyl-Asn. Compounds ML2 and ML9 were highly potent ($K_i = 30$ and 63 nM, respectively) and highly species-selective (121-fold and >1590-fold selectivity, respectively).

To improve upon ML9, we took advantage of prior work demonstrating that the Mtb20S S1 site prefers larger P1 aromatic residues than does the S1 site in c-20S.⁸ We therefore designed and synthesized (Scheme S1) the two ML9 analogues DPLG-2 and DPLG-4. In DPLG-2, a naphthyl group is incorporated into P1, while P1 in DPLG-4 contains an isopropyl substitution to test whether the S1 binding site can tolerate bulkier substituents at the 4-position of the P1 phenyl ring (Figure 1). Each maintains the *N,N*-diethyl-Asn amide as P3. DPLG-2 showed a 4-fold increase in potency ($K_i = 15$ nM) against Mtb20SOG relative to ML9; however, DPLG-4 ($K_i = 770$ nM vs Mtb20SOG) showed

~18-fold lower potency than ML9, indicating that the bulky group at the 4-position of the P1 phenyl ring is not tolerated well by the S1 pocket of the Mtb proteasome.

Contrary to the rapid-equilibrium inhibition shown by ML9,¹⁴ DPLG-2 inhibited Mtb20SOG in a time-dependent manner (Figure 2A). Mtb20OG (48 nM) was preincubated with and fully inactivated by DPLG-2 (2.5 μM) and then diluted into buffer containing substrate, and the recovery of the activity was recorded for ~25 min (Figure S2). The recovery data points were fitted to eq 1 to determine the dissociation rate constant, which was found to be $k_{\text{off}} = 0.0015 \pm 0.0001 \text{ s}^{-1}$, indicating that the half-life of the enzyme-inhibitor complex is 7.7 min. To determine the apparent association rate constant (k_{on}), proteolytic reaction progress curves in the presence of DPLG-2 at various concentrations were recorded (Figure 2B), and the data points were fitted to eq 1 to determine k_{obs} at each inhibitor concentration. Plotting k_{obs} against the inhibitor concentration and fitting to eq 2 (Figure 2C) gave $k_{\text{on}} = (5.7 \pm 0.2) \times 10^4 \text{ M}^{-1} \text{ s}^{-1}$. The apparent inhibition constant of DPLG-2 against Mtb20SOG was determined to be $K_i^{\text{app}} = 24.2 \pm 0.9$ nM by plotting the reaction rate ratio v_i/v_0 against the inhibitor concentration and fitting to eq 3 (Figure 2D). This agreed well with the value of 26.3 nM calculated using $K_i^{\text{app}} = k_{\text{off}}/k_{\text{on}}$. The K_i value of 15 nM was calculated using eq 4. DPLG-2 was 4-fold more potent against Mtb20SOG than ML9 and showed greater species selectivity (4670-fold selectivity using $K_i = 70 \mu\text{M}$ vs human c-20S) (Table 2). The underlying reason for the change

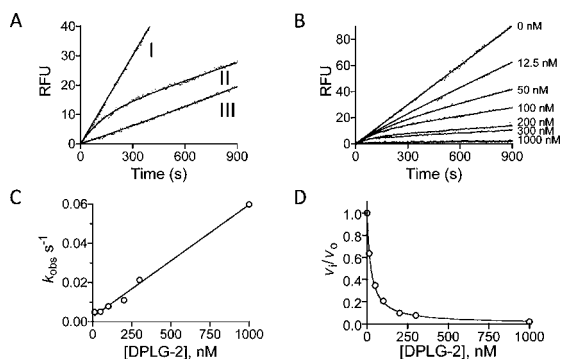


Figure 2. DPLG-2 is a time-dependent inhibitor of Mtb20S. (A) Proteolytic activity of Mtb20SOG (0.28 nM) with substrate suc-LLVY-AMC (50 μ M) alone (curve I) or following the addition of DPLG-2 (curve II) or ML9 (curve III) at 100 nM. (B) Progress curves for hydrolysis of suc-LLVY-AMC by Mtb20SOG in the presence of various concentrations of DPLG-2 to determine k_{obs} . Solid curves are fits to eq 1. (C) Plot of k_{obs} vs DPLG-2 concentration to determine k_{on} . The solid line is a fit to eq 2. (D) Plot of v_i/v_0 vs inhibitor concentration to determine K_i^{app} . The solid curve is a fit to eq 3.

Table 2. Selectivities of ML2, ML9, and DPLG-2 for Mtb over Human c-20S β 5c and i-20S β 5i

ID	K_i (μ M)			$K_{i(\beta 5i)}/K_{i(\text{Mtb})}$	
	Mtb20SOG	β 5c	β 5i	β 5c	β 5i
ML2	0.030	3.63	0.82	121	27
ML9	0.063	>100	26.3	>1590	417
DPLG-2	0.015	70	54.7	4670	3650

in the mechanism from rapid-equilibrium to slow-binding inhibition is under investigation.

$$[P] = v_s t + \frac{(v_i - v_s)}{k_{\text{obs}}}(1 - e^{-k_{\text{obs}} t}) \quad (1)$$

$$k_{\text{obs}} = k_{\text{on}}[I] + k_{\text{off}} \quad (2)$$

$$\frac{v_i}{v_0} = \frac{1}{1 + [I]/K_i} \quad (3)$$

$$K_i = \frac{K_i^{\text{app}}}{1 + [S]/K_M} \quad (4)$$

The availability of crystal structures allowed us to compare the binding pockets of Mtb20S and eukaryotic proteasomes. As shown in Figure 3, the S3 binding pocket of Mtb20S differs significantly from those of yeast 20S and mouse c-20S and i-20S. The P3 neopentylasparagine residue of ML16 fits perfectly in the S3 sites of the mammalian proteasomes (Figure 3A,C,D) but poorly in the S3 site of the Mtb proteasome (Figure 3B). Although the S1 binding pockets of Mtb20S and c-20S are substantially different, those of Mtb20S and i-20S are similar, and both proteasomes prefer larger aromatic groups at the P1 position of the *N*-acetyl tripeptide-AMC substrate (Figure S3).^{8,14} To test whether dipeptides that are selective for the Mtb proteasome over the human constitutive proteasome are comparably poor inhibitors of human i-20S, we measured IC_{50} 's for selected compounds and converted them to K_i 's as described above (Table 2). In agreement with the structural analysis, ML9 and DPLG-2 inhibited human i-20S β 5i poorly ($K_i = 26.3$ and 54.7μ M, respectively). However, ML2 showed potent inhibitory activity against i-20S ($K_i = 0.82 \mu$ M). Since both ML9 and

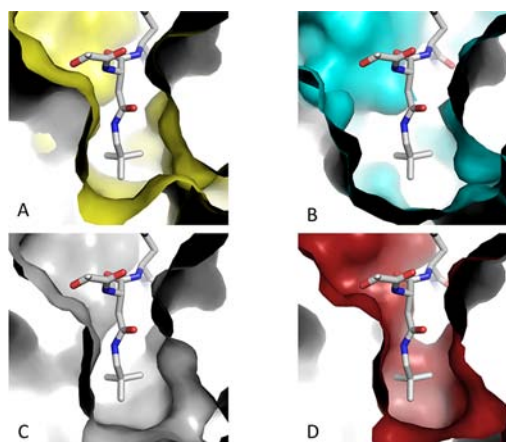


Figure 3. Comparison of the S3 binding pockets of yeast c-20S, Mtb20S, mouse c-20S, and mouse i-20S. The solved cocystal structure of yeast 20S and ML16 (3MG8) is shown in (A), while Mtb20S (2FHG) in (B), mouse c-20S (3UNB) in (C), and mouse i-20S (3UNF) in (D) are superimposed on the solved structure. Figures were made using MacPyMOL (DeLano Scientific, Palo Alto, CA).

DPLG-2 have the P3 *N,N*-diethylamide moiety whereas ML2 has a much less bulky P3 pyrrolidinylamide moiety, these results indicate that the S3 binding pocket dictates the species selectivity for Mtb20S over both human c-20S and i-20S and that an acyclic, fully substituted Asn side chain is required for selectivity against both c-20S and i-20S. The shift to a slow-binding mechanism suggests that binding may stabilize an altered conformation. Consistent with this, the P1 naphthyl moiety cannot be docked into the crystallographically determined S1 pocket of Mtb20S (Figure S4).

To test whether the dipeptides are mycobactericidal toward nonreplicating Mtb under nitrosative stress, we incubated Mtb in 0.5 mM NaNO_2 at pH 5.5 in Sauton's medium overnight and then added the dipeptides at indicated concentrations for 5 or 11 days (Figure 4A). ML2, ML9, and DPLG-2 were cidal, with up to 1 \log_{10} reduction in colony-forming units after 5 days and up to 2.2 \log_{10} of killing after 11 days at concentrations that were greater than twice their K_i 's. Above 100 nM, there was no significant increase in the extent of killing when the concentrations of the inhibitors were increased to 25 μ M. Killing was dependent on dose (Figure 4A inset), nitrosative stress (Figure S5A,B), and *prcBA* (Figure S5C). The incomplete extent of killing phenocopied the Mtb *prcBA* knockout over the same time period under nonreplicating conditions.⁶ The fact that the bacteria were not completely eradicated mirrors the action of many other compounds that are active on nonreplicating Mtb, such as a DlaT inhibitor¹⁵ and rifampin (data not shown). As discussed in the SI, treatment with *N,C*-capped dipeptides did not phenocopy *prcBA* deficiency completely, perhaps because the dipeptides did not inhibit the proteasome completely. In contrast to 1,3,4-oxathiazol-2-ones, DPLG-2 was stable in human plasma over 22 h (Figure S6).

The ability to kill Mtb provided strong evidence that the dipeptides entered the bacteria, but this would have been difficult to confirm by testing for proteasome inhibition in lysates prepared from dipeptide-treated Mtb because binding would have been reversed when the cells were washed and lysed. To circumvent this problem, we devised a competition assay using HT1171, an oxathiazolone that can enter Mtb and inhibit its proteasome irreversibly.⁹ We reasoned that if the dipeptides could prevent the inhibition of the Mtb proteasome inside intact

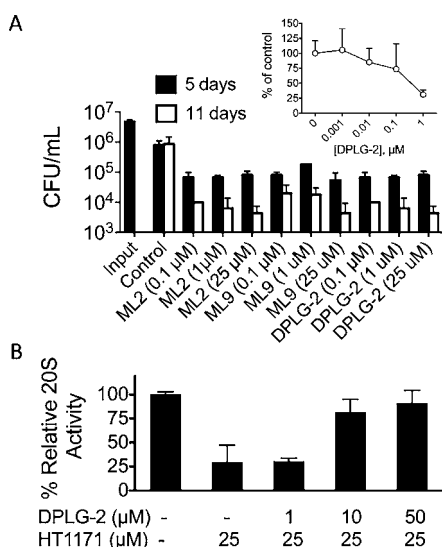


Figure 4. N,C-dipeptides inhibit mycobacterial proteasomes and kill nonreplicating Mtb. (A) Killing of Mtb H37Rv in Sauton's medium with 0.5 mM NaNO₂ at pH 5.5, which mimics the nitrosative stress that limits the replication of Mtb in mice.¹⁰ Data are means of triplicates of at least three experiments. Inset: DPLG-2 kills Mtb in the presence of NaNO₂ at pH 5.5 in a dose-dependent manner. (B) BCG cells were incubated with DPLG-2 at the indicated concentrations for 4 h prior to addition of HT1171 and then incubated for an additional hour. Proteasome activity in lysates was tested with suc-LLVY-AMC as the substrate. Data are means of triplicates of three experiments.

mycobacteria by HT1171, this would indicate that the dipeptides had penetrated the mycobacteria and bound to the proteasome active site. Mid-log-phase cells of *Mycobacterium bovis* strain BCG were incubated with DPLG-2 at the indicated concentrations for 4 h prior to addition of HT1171 (25 μM) and then incubated for a further 1 h, after which the cells were washed extensively to remove unbound inhibitors of both types. The proteasomal activities of the lysates (Figure 4B) were determined as reported elsewhere.⁹ In the absence of DPLG-2 or in the presence of concentrations of DPLG-2 (1 μM) that were low relative to HT1171 (25 μM), HT1171 inhibited the proteasomes irreversibly. However, DPLG-2 at 10 or 50 μM was able to shield the mycobacterial proteasome active sites from HT1171. Thus, DPLG-2 can penetrate mycobacteria and bind to proteasome active sites in situ. Efforts to conduct a similar competition experiment with Me4BodipyFL-Ahx3Leu3VS were not possible, as that probe afforded only 8% inhibition of the Mtb proteasome, in accord with earlier work.⁸

In summary, we have identified a series of N,C-capped dipeptides that are highly selective for the Mtb proteasome over both human constitutive and human immunoproteasomes and can penetrate Mtb to exert cidal activity against nonreplicating bacteria under nitrosative stress. After oxathiazolones, N,C-capped dipeptides are only the second class of compounds to show a high degree of selectivity for the proteasome of a pathogen over that of its host. Selectivity was achieved in a novel way by exploiting two facts: (1) the S3 binding pocket is shallow and wide between two β subunits in Mtb20S but narrow and deep between β5/β5i and β6 in c-20S/i-20S, and (2) the S1 binding pocket accommodates large aromatic rings in Mtb20S but not in human c-20S. A further novelty emerged within the class of N,C-capped dipeptides in that replacement of the P1 phenyl ring with a naphthyl substituent changed the inhibition modality from rapid equilibrium to a time-dependent mechanism

and increased the residence time of the inhibitor in its binding site, an important goal in drug development for non-covalent inhibitors.

■ ASSOCIATED CONTENT

Supporting Information

Methods and additional data. This material is available free of charge via the Internet at <http://pubs.acs.org>.

■ AUTHOR INFORMATION

Corresponding Author

gal2005@med.cornell.edu; cnathan@med.cornell.edu.

Notes

The authors declare no competing financial interest.

■ ACKNOWLEDGMENTS

We thank Xiuju Jiang for BSL3 technical support. This work was supported by NIH (R56AI080618 to C.N. and 1R21AI101393 to G.L.) and the Milstein Program in Chemical Biology of Infectious Diseases. The Department of Microbiology and Immunology is supported by the William Randolph Hearst Foundation.

■ REFERENCES

- (1) Baumeister, W.; Walz, J.; Zuhl, F.; Seemuller, E. *Cell* **1998**, *92*, 367.
- (2) (a) Brown, M. G.; Driscoll, J.; Monaco, J. J. *Nature* **1991**, *353*, 355. (b) Glynne, R.; Powis, S. H.; Beck, S.; Kelly, A.; Kerr, L. A.; Trowsdale, J. *Nature* **1991**, *353*, 357. (c) Kelly, A.; Powis, S. H.; Glynne, R.; Radley, E.; Beck, S.; Trowsdale, J. *Nature* **1991**, *353*, 667.
- (3) Kincaid, E. Z.; Che, J. W.; York, I.; Escobar, H.; Reyes-Vargas, E.; Delgado, J. C.; Welsh, R. M.; Karow, M. L.; Murphy, A. J.; Valenzuela, D. M.; Yancopoulos, G. D.; Rock, K. L. *Nat. Immunol.* **2012**, *13*, 129.
- (4) Lin, G.; Hu, G.; Tsu, C.; Kunes, Y. Z.; Li, H.; Dick, L.; Parsons, T.; Li, P.; Chen, Z.; Zwickl, P.; Weich, N.; Nathan, C. *Mol. Microbiol.* **2006**, *59*, 1405.
- (5) Darwin, K. H.; Ehrhart, S.; Gutierrez-Ramos, J. C.; Weich, N.; Nathan, C. F. *Science* **2003**, *302*, 1963.
- (6) (a) Gandotra, S.; Lebron, M. B.; Ehrhart, S. *PLoS Pathogens* **2010**, *6*, No. e1001040. (b) Gandotra, S.; Schnappinger, D.; Monteleone, M.; Hillen, W.; Ehrhart, S. *Nat. Med.* **2007**, *13*, 1515.
- (7) Nathan, C.; Gold, B.; Lin, G.; Stegman, M.; de Carvalho, L. P.; Vandal, O.; Venugopal, A.; Bryk, R. *Tuberculosis* **2008**, *88* (Suppl. 1), S25.
- (8) Lin, G.; Tsu, C.; Dick, L.; Zhou, X. K.; Nathan, C. *J. Biol. Chem.* **2008**, *283*, 34423.
- (9) Lin, G.; Li, D.; de Carvalho, L. P.; Deng, H.; Tao, H.; Vogt, G.; Wu, K.; Schneider, J.; Chidawanyika, T.; Warren, J. D.; Li, H.; Nathan, C. *Nature* **2009**, *461*, 621.
- (10) MacMicking, J. D.; North, R. J.; LaCourse, R.; Mudgett, J. S.; Shah, S. K.; Nathan, C. F. *Proc. Natl. Acad. Sci. U.S.A.* **1997**, *94*, 5243.
- (11) Nathan, C. *Science* **2006**, *312*, 1874.
- (12) Kruger, E.; Kloetzel, P. M. *Curr. Opin. Immunol.* **2012**, *24*, 77.
- (13) Huber, E. M.; Basler, M.; Schwab, R.; Heinemeyer, W.; Kirk, C. J.; Groettrup, M.; Groll, M. *Cell* **2012**, *148*, 727.
- (14) Blackburn, C.; Gigstad, K. M.; Hales, P.; Garcia, K.; Jones, M.; Bruzzese, F. J.; Barrett, C.; Liu, J. X.; Soucy, T. A.; Sappal, D. S.; Bump, N.; Olhava, E. J.; Fleming, P.; Dick, L. R.; Tsu, C.; Sintchak, M. D.; Blank, J. L. *Biochem. J.* **2010**, *430*, 461.
- (15) Bryk, R.; Gold, B.; Venugopal, A.; Singh, J.; Samy, R.; Pupek, K.; Cao, H.; Popescu, C.; Gurney, M.; Hotha, S.; Cherian, J.; Rhee, K.; Ly, L.; Converse, P. J.; Ehrhart, S.; Vandal, O.; Jiang, X.; Schneider, J.; Lin, G.; Nathan, C. *Cell Host Microbe* **2008**, *3*, 137.